ELSEVIER

Nanomedicine: Nanotechnology, Biology, and Medicine
45 (2022) 102589

nanomedicine
Nanotechnology, Biology, and Medicine

nanomedjournal.com

Lipoplexes for effective *in vitro* delivery of microRNAs to adult human cardiac fibroblasts for perspective direct cardiac cell reprogramming

Letizia Nicoletti, MSc[a,1], Camilla Paoletti, PhD[a,1], Giulia Tarricone, MSc[a,2], Ilaria Andreana, PhD[b], Barbara Stella, Professor[b], Silvia Arpicco, Professor[b], Carla Divieto, PhD[c], Clara Mattu, PhD[a,3], Valeria Chiono, Professor[a,3,*]

[a]*Department of Mechanical and Aerospace Engineering, Politecnico di Torino, Corso Duca degli Abruzzi 24, 10129 Turin, Italy*
[b]*Department of Drug Science and Technology, University of Turin, Via Pietro Giuria, 11, 10125, Turin, Italy*
[c]*Istituto Nazionale di Ricerca Metrologica, Division of Advanced Materials and Life Sciences, Str. delle Cacce, 91, 10135 Turin, Italy*

Revised 23 June 2022

Abstract

Design of nanocarriers for efficient miRNA delivery can significantly improve miRNA-based therapies. Lipoplexes based on helper lipid, dioleoyl phosphatidylethanolamine (DOPE) and cationic lipid [2-(2,3-didodecyloxypropyl)-hydroxyethyl] ammonium bromide (DE) were formulated to efficiently deliver miR-1 or a combination of four microRNAs (miRcombo) to adult human cardiac fibroblasts (AHCFs). Lipoplexes with amino-to-phosphate groups ratio of 3 (N/P 3) showed nanometric hydrodynamic size (372 nm), positive *Z*-potential (40 mV) and high stability under storage conditions. Compared to commercial DharmaFECT1 (DF), DE-DOPE/miRNA lipoplexes showed superior miRNA loading efficiency (99 % *vs.* 64 %), and faster miRNA release (99 % *vs.* 82 % at 48 h). DE-DOPE/miR-1 lipoplexes showed superior viability (80–100 % *vs.* 50 %) in AHCFs, a 2-fold higher miR-1 expression and Twinfilin-1 (TWF-1) mRNA downregulation. DE-DOPE/miRcombo lipoplexes significantly enhanced AHCFs reprogramming into induced cardiomyocytes (iCMs), as shown by increased expression of CM markers compared to DF/miRcombo.

Keywords: Adult human cardiac fibroblasts; Lipoplexes; miRcombo; microRNAs; Direct reprogramming

Background

MicroRNAs (miRNAs) are small endogenous single-strand non-coding RNAs of nearly 21 nucleotides, that function as guide molecules in post-transcriptional regulation of gene expression.[1] MiRNAs biogenesis takes place at multiple steps. In animals, miRNA genes are transcribed by RNA polymerase II and further processed by two ribonuclease III proteins, Drosha and Dicer, which work in the nucleus and in the cytoplasm, respectively.[2] Once mature, miRNAs are loaded onto an Argonaute (AGO) protein to form an effector complex called RISC (RNA induced silencing complex), leading to translational repression or cleavage and subsequent degradation of target messenger RNAs (mRNAs).

Deregulation of miRNAs expression has been reported in different pathologies, including cancer, cardiovascular diseases and neurological disorders, paving the way to the development of several miRNA-based therapies.[3–6] According to the deregulation status of the target mRNAs, these therapies can be classified as: i) miRNA gain-of-function therapy, which restores the expression by using chemically modified double-stranded miRNA mimics; and ii) miRNA suppression therapy, which inhibits endogenous miRNA expression using miRNAs antagonists (anti-miRs) or inhibitors.[7] Moreover, therapies based on the simultaneous delivery of different miRNA combinations are under investigation, to maximize treatment efficacy by exploiting their synergistic action.[8,9]

Despite the great potential of miRNA-based therapies, their clinical translation is made difficult by the nature of the

* Corresponding author at: Politecnico di Torino, DIMEAS, C.so Duca degli Abruzzi 24, 10129 Torino, Italy.
E-mail address: valeria.chiono@polito.it (V. Chiono).
[1] These authors contributed equally to this work.
[2] **Present Address:** Italian Institute of Technology, Genoa, Italy.
[3] Co-last authors.

https://doi.org/10.1016/j.nano.2022.102589

therapeutic molecules, which suffer from fast degradation rate and poor *in vivo* half-life.[10] Furthermore, naked miRNAs cannot spontaneously enter the cells due to the electrostatic repulsion between the negatively charged miRNAs and cell membrane. Thus, proper carriers should be designed to improve the transport kinetics of miRNA therapeutics, facilitate their on-target accumulation, and enhance cell membrane by-passing. Nano-size delivery vehicles of various composition and structure have been proposed for this purpose, by virtue of their ability to extend circulation time, reduce clearance, and enhance cellular uptake of their payload[10,11]

Cell delivery of miRNAs with viral vectors, lipid-based transfection agents, as well as synthetic and natural polymer-based nanoparticles (NPs) has been reported.[12–14] Viral vectors (such as retroviruses, lentiviruses, and adenoviruses) have been widely used to deliver miRNAs to cells by virtue of their high transfection efficiency, but suffer from serious drawbacks, such as toxicity, adverse immune response and consequent inflammatory activation.[15,16] Besides, high-quality viral vectors are difficult to be scaled up.

In light of these considerations, inorganic and organic non-viral vehicles based on gold or silica nanoparticles, lipids, polymers, micelles and exosomes have been explored, being safer and easier to manufacture and scale up.[15] Among them, cationic lipids have demonstrated the ability to establish strong and spontaneous electrostatic interactions with opposite-charged miRNAs.[17,18] A great variety of different cationic lipids, such as 2,3-dioleyloxy-N-[2(sperminecarboxamido)ethyl]-*N*,*N*-dimethyl-l-propanaminium trifluoroacetate (DOSPA) and dioctadecylamidoglycylspermine (DOGS), in combination with the neutral fusogenic phospholipid, dioleoyl phosphatidylethanolamine (DOPE), have been proposed.[17,19,20,21] The formation of complexes between cationic lipids and miRNAs, called lipoplexes, enables efficient cargo protection from enzymatic degradation and facilitates the interaction with the negatively charged cell membrane, enhancing miRNA delivery into cells without triggering pathogenic or immunogenic responses.[14,22,23] Because of these interesting properties, cationic lipids are present in the formulation of several commercially available transfection reagents used for *in vitro* miRNA delivery, such as Lipofectamine® RNAi-MAX,[24] SiPORT™ (Invitrogen),[25] SilentFect™ (Bio-Rad)[26] and DharmaFECT® (Dharmacon).[27,28,29] These commercial transfection reagents have demonstrated high loading and transfection efficiency depending on the cell type.[24,30,31] For instance, the transfection efficiency of Lipofectamine 3000 is reported to be ~97 % in primary muscle myoblasts, and as low as ~25 % in HepG2 Liver cancer cells.[24] However, considering that cytotoxicity remains one major limitation of lipidic transfectants,[24] the design of safer and more cytocompatible transfection reagents is highly demanded.

Herein, we report on the preparation and characterization of biocompatible lipoplexes, able to efficiently load single miRNA and miRNA combinations (miRcombo) and deliver them to adult human cardiac fibroblasts (AHCFs), for perspective applications in direct reprogramming of AHCFs into induced cardiomyocytes (iCMs).[29] The designed lipid formulation, based on DOPE and the cationic lipid [2-(2,3-didodecyloxypropyl)-hydroxyethyl] ammonium bromide (DE) has previously shown high siRNA and plasmid DNA transfection efficiency but has not been exploited for miRNA delivery so far.[32–38] In this work, DE-DOPE/miRNA lipoplexes were prepared and characterized for their ability to deliver miRNAs (single miRNA and miRcombo) to AHCFs compared to commercial DharmaFECT (DF), as it has been frequently used as transfection agent for miRcombo in direct cardiac reprogramming.[31,32] DE-DOPE/miRNA lipoplexes were prepared *via* spontaneous electrostatic interactions, modulating the Iratio between the positively charged groups on the cationic lipid (N) and the negatively charged groups on miRNA (P) to obtain lipoplexes with positive *Z*-potential, nanometric size, sufficient stability under storage conditions and adequate stability under physiological conditions for efficient miRNA delivery to cells. DE-DOPE/miRNA lipoplexes showed enhanced biocompatibility, ~99 % miRNA loading efficiency and ability to fully deliver the miRNA cargo to AHCFs, resulting in significantly higher expression of GATA4, MEF2C, TNNT2 and ACTC1 mRNA as compared to control DF-based lipoplexes. Our findings indicate that DE-DOPE/miRNA lipoplexes are ideal systems for *in vitro* microRNA-delivery, and promising carriers for miRcombo-mediated direct reprogramming of human cardiac fibroblasts into iCMs. This work highlights the key role of a multidisciplinary research, exploiting bioengineering and nanotechnology tools, in addressing the barriers to successful non-viral direct cardiac reprogramming, including those arising from inefficient miRNA delivery.

Materials

ICationic lipid [2-(2,3-didodecyloxypropyl)-hydroxyethyl] ammonium bromide (DE) was synthesized as previously described.[32] L-alpha-dioleoylphosphatidylethanolamine (DOPE) and chloroform were purchased from Sigma. DharmaFECT1 (DF; Dharmacon™) was supplied from Horizon Discovery.

ITrackIt™ 50 bp DNA Ladder, TAE Buffer (Tris-acetate-EDTA) (50×), SYBR™ Green I Nucleic Acid Gel Stain - 10,000× concentrated in dimethyl sulfoxide (DMSO) for agarose gel electrophoresis were purchased from Life Technologies. Qubit™ microRNA Assay Kit and agarose low-EEO were supplied from Thermo Fisher Scientific. Phosphate buffer solution (PBS 10×, pH 7.4) was purchased from Gibco. In the following, water refers to ultra-purified Milli-Q water (Millipore).

NegmiR (mirVana™ miRNA Mimic, Negative Control #1), miR-1-3p, miR-133a-3p, miR-208a-3p, and miR-499a-5p (mirVana™ miRNA mimic) and FAM™-labeled miR-1 (mirVana miRNA mimic) were purchased from Life Technologies. Adult Human Cardiac Fibroblasts (AHCFs, CC-2903) and Fibroblasts Growth Medium-3 (CC-4526) were purchased from Lonza. Dulbecco's modified Eagle Medium (DMEM) High Glucose and 0.25 % w/v trypsin/EDTA were purchased from Gibco. Fetal bovine serum (FBS), L-glutamine, Formalin Free Tissue Fixative, 4′,6-diamidino-2-phenylindole (DAPI) and penicillin/streptomycin/ampicillin were supplied from Sigma. Qiazol lysis reagent, miRCURY LNA RT Kit, (hsa-miR-1-3p miRCURY LNA miRNA PCR Assay) were purchased from Qiagen. EvaGreen supermix, ddPCR supermix for probes without dUTP, TWF-1, GATA4, ME2C, TNNNT2 and ACTC1 and glyceraldehyde 3-phosphate dehydrogenase (GAPDH) were

purchased from Bio-Rad Laboratories. Resazurin was supplied from Promega. Nuclease-free water was supplied from Fisher Bioreagents.

Methods

Preparation of liposomes and miRNA lipoplexes

IEmpty DE-DOPE liposomes were prepared using the thin lipid film-hydration method.[41] The cationic lipid DE and helper lipid DOPE were dissolved separately in chloroform and mixed in a 1:1 ratio (w/w). The mixture was then dried under reduced pressure in a rotary evaporator. Residual traces of chloroform were removed by placing the vials under high vacuum for one hour. The lipid film was hydrated with Milli-Q water to a final concentration of 1 mg/mL of lipids, under vortex stirring, until complete film detachment and formation of a liposomal suspension.

Lipoplexes containing negmiR were prepared at different DE-DOPE/miRNA ratios, by changing the amino to phosphate groups (N/P) molar ratio (3; 1.75; 0.7; 0.35). Briefly, to obtain DE-DOPE/miRNA lipoplexes with different N/P ratios (as detailed in Supplementary Table S1), a constant amount of miRNA (0.7 μg corresponding to 10 μL of miRNA solution with 5 μM concentration) and different amounts of DE-DOPE were mixed and incubated for 20 min at room termperature, vortexed and then incubated for additional 20 min. Lipoplexes were diluted in Milli-Q water to a final volume of 1 mL. DF/miRNA lipoplexes were obtained by following the manufacturer's instructions by preliminary optimization of the DF/miRNA ratio (Supplementary Material). Based on that, miRNA (0.7 μg) and DF (6 μg) were diluted in separate tubes in Milli-Q water or in serum free-medium for cell studies to a final volume of 200 μL, and, then, the content of each tube was incubated for 5 min at room temperature. Afterwards, the miRNA solution was added to DF, mixed by pipetting carefully up and down and incubated for additional 20 min at room temperature.

DE-DOPE lipoplexes at N/P 3 ratio and DF/miRNA lipoplexes were also loaded with functional miR-1 and miRcombo for *in vitro* cell studies, using the same formulation protocol reported above.

Physical and chemical characterization

Size and surface charge

Size distribution, polydispersity index (PDI) and surface charge of liposomes and lipoplexes were analyzed by dynamic light scattering (DLS) using a Litesizer™ 500 (Anton Paar, Turin, Italy). DLS analysis was carried out by backscatter detection with a scattering angle of 173°. The surface charge of liposomes and lipoplexes was evaluated by zeta potential measurements using a U-shaped fold capillary cell (Anton Paar, Turin, Italy). All measurements were carried out in triplicate.

Stability

The physical stability of lipoplexes at physiological temperature was evaluated by measuring their size, polydispersity index and zeta potential as a function of their incubation time (0, 4, 6, 24 and 48 h) at 37 °C in Milli-Q water. Similarly, the stability of lipoplexes under storage conditions was evaluated by analysing their size, polydispersity index and zeta potential, after 2 and 7 days at 4 °C in Milli-Q water. DF formulations were similarly tested for comparison. All measurements were performed in triplicate.

Morphology

IMorphology of liposomes and lipoplexes was analyzed by cryogenic-transmission electron microscopy (cryo-TEM), using a Philips CM120 microscope (Philips, Amsterdam, The Nederland) at the "Centre Technologique des Microstructures" (CTμ) at the Université Claude Bernard Lyon 1 (Villeurbanne, France). The diluted samples were dropped onto 300 Mesh holey carbon films (Quantifoil R2/1) and quench-frozen in liquid ethane using a cryo-plunge workstation (made at LPS Orsay). The specimens were then mounted on a precooled Gatan 62 specimen holder and observed at an accelerating voltage of 120 kV.

Loading efficiency (LE)

The miRNA loading efficiency of lipoplexes was determined by an indirect method through the measurement of free miRNA concentration in water after lipoplex preparation. Briefly, miRNA-loaded lipoplexes were centrifuged (15,000 rpm, 15 min at 4 °C) using an Allegra X30 benchtop centrifuge (Beckman Coulter, Brea, California, USA). Supernatants were collected and analyzed by benchtop Qubit™ 4 Fluorometer following manufacturer's instructions (Life Technologies, Carlsbad, California, USA). This method allows accurate miRNA quantification by fluorescence-based detection. For miRNA loading evaluation, 10 μL of the supernatant containing non-loaded miRNA were added to 190 μL of working solution (obtained by diluting Qubit® microRNA reagent in Qubit® microRNA buffer 1:200) and mixed for 2–3 s. The mixture was incubated for 2 min in the dark and analyzed by Qubit® 3.0 Fluorometer's RNA detection program. Loading efficiency was calculated using the following equation (Eq. (1)):

$$LE\,(\%) = \frac{Total\ miRNA – free\ miRNA\ in\ supernatant}{Total\ miRNA} \times 100 \quad (1)$$

where total miRNA is the amount of miRNA used for lipoplex preparation.

The amount of miRNA molecules in a single DE-DOPE/miRNA and DF/miRNA lipoplex was determined by the following equation (Eq. (2)), as described by H. Yang et al.[42]:

$$[\text{miRNA/lipoplex}] = \frac{miRNA\ molar\ concentration}{total\ lipoplexes\ molar\ concentration} \quad (2)$$

where the total miRNA concentration was determined by considering LE, while the total lipoplex concentration was determined according to Eq. (3):

$$[Total\ lipoplex\ molar\ \ concentration] = \frac{\frac{Number\ of\ lipoplexes}{Avogadro's\ number}}{Volume\ of\ lipoplex\ \ suspension} \quad (3)$$

And

$$Number\ of\ lipoplexes = \frac{Total\ volume\ of\ \ lipoplexes}{Average\ volume\ of\ each\ lipoplex} = \frac{\frac{g\ of\ \ lipoplexes}{density\ of\ lipoplexes\left(\frac{g}{cm^3}\right)}}{\frac{4}{3}\left(lipoplex\ radius\ in\ nm \times 10^{-7}\right)^3} \quad (4)$$

The density of lipoplexes was approximated to the density of water (1 g/cm^3) due to the their stability in Milli-Q water.

The loading of miRNA was also qualitatively investigated by agarose gel electrophoresis (30 min; 100 V), as previously described.[43] Briefly, 10 μL of supernatant, collected after lipoplex formulation, was mixed with 2 μL 6× TrackIt™ Cyan/Orange loading buffer, reaching a final volume of 12 μL (Invitrogen, Waltham, Massachusetts, USA). The suspension was then loaded onto 2 % agarose gel in TAE 1× buffer containing SYBR® Green for nucleic acid staining. The images were visualized after UltraBright LED Transilluminator (Maestrogen, Hsinchu City, Taiwan) exposure (470 nm). Free miRNA, DF formulations and DE-DOPE liposomes were analyzed as controls. TrackIt 50 bp DNA Ladder was used as marker.

miRNA release

To evaluate the release kinetics of miRNA, lipoplexes were incubated in 10 mM PBS at 37 °C for different time intervals (1, 2, 3, 4, 6, 8, 24 and 48 h). A volume of 15 μL was collected and analyzed by Qubit™ 4 Fluorometer as described above and replaced with 15 μL fresh PBS. The amount of released miRNA was calculated as the ratio between miRNA released at each time interval and the total amount of miRNA loaded in the lipoplexes. miRNA release was also qualitatively investigated by agarose gel electrophoresis, following the same protocol described above. Experiments were performed in triplicate. miRNA release study was also evaluated with the cationic lipid DF for comparison.

In vitro study

Cell culture

AHCFs were maintained in culture using FGM-3 containing 10 % FBS, 1 % insulin, 1 % human basal fibroblast growth factor (hFGF-) and 1 % gentamicin. Cells were expanded until passage 4 and then used for experiments. Complete media made using DMEM high glucose supplemented with 10 % FBS and 1 % L-glutamine was used for all experiments.

Viability assay

For viability assay, AHCFs were seeded in 96-well plate (6×10^3 cells/well) in complete media 24 h before transfection. The next day, cells were transfected with empty DF and DE-DOPE liposomes or their miR-1 loaded lipoplexes, by combining proper volume of each formulation (Supplementary Table S1 and Table 1) with complete media reaching 100 μl volume per well. For DE-DOPE liposomes and lipoplexes, different concentrations were tested by diluting the original formulation (DE-DOPE/miRNA_100), as detailed in Table 1. After 24 h from transfection, the medium was replaced with complete media, and culture was continued up to 48 h. Non-transfected cells were analyzed as control. Cell viability was assessed after 24 and 48 h culture time. Resazurin was prepared at a final concentration of 40 μM in complete culture media and added to transfected cells after each time interval. Cells were then incubated for 3 h. Fluorescence reading (Ex = 550 nm/ Em = 590 nm) was performed using NanoQuant plate (Tecan Group Ltd., Männedorf, Svizzera). Cell viability was reported as percentage of viable cells relative to control (untreated) cells. To aquire brightfield images, AHCFs were seeded and cultured in 96-well plate (6×10^3 cells/well) in complete media for 24 h, then they were transfected with DF/negmiR or DE-DOPE/negmiR lipoplexes for 24 h and, finally, they were observed under a ZOE microscope (Bio-Rad). Experiments were performed in biological triplicate.

Uptake efficiency

MiRNA uptake efficiency of cells mediated by DF or DE-DOPE lipoplexes was assessed by flow cytometry and fluorescence microscopy analyses. AHCFs were plated in 24-well plates (2.2×10^4 cells/well) or in 35 mm μ-Dishes (Ibidi, 3×10^4 cell/well) for flow cytometry or fluorescence microscopy analyses, respectively, in complete media for 24 h. Cells were then transfected with miR-1 or FAM™-labeled miR-1 using DF or DE-DOPE lipoplexes, as described above, in complete media. Non-treated cells were used as control. Uptake efficiency was evaluated after 12 h of treatment. For flow cytometry, cells were washed with PBS and detached with 0.25 % w/v trypsin/EDTA, centrifuged and resuspended in MilliQ H_2O. Flow cytometry was performed using Guava Easy Cyte (Luminex Corporation, Austin, Texas, USA) flow cytometer and analyzed using GuavaSoft 3.2 software (Luminex Corporation, Austin, Texas, USA). Experiments were performed in triplicate. For fluorescence microscope images, after 12 h of treatment, cells were washed with PBS and fixed with Formalin Free Tissue Fixative for 10 min at RT and washed with PBS. Nuclei were counterstained with DAPI for 5 min at RT. Images were acquired using Nikon Eclipse Ti2 spinning disk microscope and NIS-Elements software (Nikon, Minato, Tokyo, Japan). Merge was performed using ImageJ (Fiji) software.

Cell transfection for RNA isolation

To study miRNA internalization and mRNA target down-regulation, cells were plated in 6-well plates (1.1×10^5 cells/well) in DMEM High Glucose with 10 % FBS and 1 % L-glutamine one day before transfection. This medium was used in

Table 1
Tested DE-DOPE/miRNA lipoplex formulations and corresponding miRNA concentration.

DE-DOPE/miRNA code	% of original formulation	miRNA final dose (nM)
DE-DOPE/miRNA_ 100	100 %	25
DE-DOPE/miRNA_ 65	65 %	16.25
DE-DOPE/miRNA_ 50	50 %	12.5
DE-DOPE/miRNA_ 25	25 %	6.25

all transfection studies. Cells were transfected with miR-1 or negmiR using DF or DE-DOPE lipoplexes, as described above, in complete culture media, in a final volume of 2 mL per well. After 24 h, transfection medium was replaced with fresh complete medium containing DMEM, 10 % FBS, 1 % glutamine and 1 % penicillin/streptomycin/ampicillin. Culture was continued up to 48 h. To study fibroblast reprogramming into iCMs, AHCFs were transfected with miRcombo (miR-1-3p, miR-133a-3p, miR-208a-3p, and miR-499a-5p) or negmiR using DF or DE-DOPE lipoplexes, as described above, in complete culture media, in a final volume of 2 mL volume per well. After 24 h, transfection medium was replaced with fresh complete medium containing DMEM, 10 % FBS, 1 % glutamine and 1 % penicillin/streptomycin/ampicillin. Culture was continued for additional 7 and 15 days.

RNA isolation

RNA was extracted using Qiazol lysis reagent, according to manufacturer's instructions. RNA quantity and quality were assessed using NanoQuant plate.

miRNA reverse transcription and droplet digital PCR

To study miR-1 uptake by cells, miRNA reverse-transcription PCR was performed using miRCURY LNA RT Kit. RNA samples were diluted to 5 ng/μL in nuclease-free water and the reaction was prepared following the manufacturer's instructions. Droplet digital PCR (ddPCR, Bio-Rad Laboratories, Hercules, California, USA) was performed to assess the expression of miR-1 (hsa-miR-1-3p) using EvaGreen supermix.[44] Droplet generation was performed according to manufacturer's instructions. Thermal-cycling conditions were: 95 °C for 5 min (1 cycle), 95 °C for 30 s and 55 °C for 1 min (40 cycles), 90 °C for 5 min (1 cycle), and a 4 °C infinite hold. PCR plate was loaded on Bio-Rad QX100 droplet reader for quantification of cDNA copies/μL (Bio-Rad Laboratories, Bio-Rad Laboratories, Hercules, California, USA). Analysis of the ddPCR data was performed by QuantaSoft analysis software (Bio-Rad Laboratories, Bio-Rad Laboratories, Hercules, California, USA). No template control with water was included in each assay. Experiments were performed in triplicate and repeated three times.

Total RNA reverse transcription and ddPCR

Total cDNA (200 ng) was obtained using high-capacity cDNA reverse transcription kit (Applied Biosystems, Waltham, Massachusetts, USA). DdPCR was performed to assess the expression of TWF-1, GATA4, ME2F, TNNT2 and ACTC1 using ddPCR supermix for probes without dUTP. Droplet generation was performed according to manufacturer's instructions. Thermal-cycling conditions were 95 °C for 10 min (1 cycle), 94 °C for 30 s and 55 °C for 30 s (40 cycles), 98 °C for 10 min (1 cycle), and a 4 °C infinite hold. DdPCR protocol continued as described above. GAPDH was used as a housekeeping gene to perform quantitative normalization. Results were reported as the concentration (cDNA copies/μL) of the gene of interest respect to the mean concentration (cDNA copies/μL) of GAPDH. No template control with water was included in each assay. Experiments were performed in triplicate and repeated three times.

Flow cytometry for reprogramming efficiency

AHCFs, transfected with negmiR or miRcombo using DE-DOPE lipoplexes were cultured for 15 days. Then, cells were trypsinized with 0.05 % Trypsin/EDTA (Sigma Aldrich) and permeabilized with 0.5 % v/v Tween 20 (Sigma-Aldrich) in PBS for 5 min. Ice cold PBS with 10 % FBS and 1 % sodium azide (Sigma Aldrich) was used for washing between each step. Cells were incubated with Cardiac Troponin T (cTnT) primary antibody (cat #701620, Invitrogen) for 1 h at 4 °C and Alexa Fluor 488-conjugated secondary antibody (ab150077, Abcam) for 1 h at 4 °C in the dark. Cells were run on Guava EasyCyte (Luminex Corporation) flow cytometer and data analysis was performed using GuavaSoft 3.2. The percentage of cTnT-positive cells was then calculated as an index of reprogramming efficiency.

Results

Optimization of lipoplexes formulation

Size and surface charge measurement

miRNA-loaded DE-DOPE liposomes (DE-DOPE/miRNA lipoplexes) were prepared at different N/P ratios (as detailed in Supplementary Table S1A), loading negmiR as a negative control to determine the optimal formulation conditions.

Empty DE-DOPE liposomes showed a mean hydrodynamic diameter of around 450 ± 19 nm and a positive *Z*-potential of 41 ± 10 mV (Supplementary Table S2), due to the protonated amino groups of DE.

By increasing the N/P ratio in DE-DOPE/miRNA lipoplexes, a decrease in the average hydrodynamic diameter was observed (Fig. 1A). The size ranged between 876 nm at N/P 0.35) and 372 nm at N/P 3 ($p = 0.0015$). Lipoplexes with intermediate N/P ratios showed a mean hydrodynamic diameter of 483 nm at N/P 0.7 and 403 nm at N/P 1.75, both significantly lower than the value obtained at N/P 0.35 ($p= 0.0070$ and $p = 0.0022$, respectively). Furthermore, a gradual shift from negative (−26 mV) to positive (+ 40 mV) *Z*-potential was observed by increasing the N/P ratio (Fig. 1B, $p < 0.0005$), suggesting that the neutralization of surface charges occurred between N/P 0.7 (−12 ± 7 mV) and N/P 1.75 (28 ± 17 mV, $p = 0.0111$).

PDI data summarized in Supplementary Table S2 indicate polydisperse formulations for empty DE-DOPE liposomes and DE-DOPE/miRNA lipoplexes at N/P 0.35. A lower PDI was measured for DE-DOPE/miRNA lipoplexes with N/P higher than 0.35, suggesting that monodisperse formulations was obtained at N/P 0.70, 1.75 and 3.

As a comparison, lipoplexes formulated with commercial DF showed a hydrodynamic diameter of 273 nm and a *Z*-potential of +54 mV (Supplementary Figure S1 and Table S3), which are comparable to the values obtained for DE-DOPE/miRNA lipoplexes at N/P 3. On the other hand, the PDI value of DF/miRNA lipoplexes (0.33 ± 0.09) was slighlty higher than that of DE-DOPE/miRNA lipoplexes with N/P 3 (0.29 ± 0.08), indicating their superior polydispersity.

Stability study

The short-term stability of DE-DOPE/miRNA lipoplexes with different N/P ratios was studied under storage conditions (*i.e.*, in water at 4 °C). The hydrodynamic diameter and the Z-

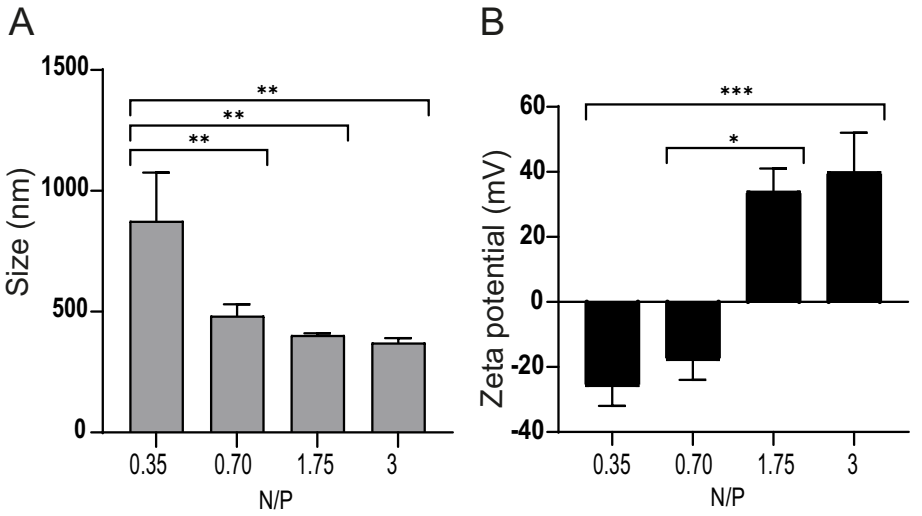

Fig. 1. (A) Hydrodynamic diameter and (B) Zeta potential of DE-DOPE/miRNA lipoplexes prepared at different DE-DOPE/miRNA (N/P) ratio, measured by DLS. NegmiR was loaded as model miRNA. Data are expressed as mean ± SD. Statistical analysis was performed by 1-way ANOVA.

potential of DE-DOPE/miRNA lipoplexes were evaluated at 2 and 7 days and are summarized in Fig. 2.

Results showed that the hydrodynamic diameter of DE-DOPE/miRNA lipoplexes with N/P 0.35 stored at 4 °C did not change significantly as a function of time, ranging between 703 nm and 891 nm. Hydrodynamic size of DE-DOPE/miRNA lipoplexes with N/P 0.70 significantly increased as a function of time, reaching a value of 703 nm after 7 days incubation. On the contrary, DE-DOPE/miRNA lipoplexes with N/P 1.75 and N/P 3 were stable up to 2 days, and a size increase was detected only after 7 days.

The surface charge variation with time was also dependent on N/P ratio. *Z*-potential was negative and approximately constant for DE-DOPE/miRNA lipoplexes with N/P 0.35 and 0.70. For DE-DOPE/miRNA lipoplexes with N/P 1.75 an inversion in the Z-potential from positive to negative values was observed between 2 and 7 days incubation ($p = 0.0385$). DE-DOPE/miRNA lipoplexes with N/P ratio of 3 were more stable and maintained a positive *Z*-potential for the whole duration of the analysis, with a non-significant decrease of the average Z-potential at day 7.

The PDI values (Supplementary Table S5) of DE-DOPE/miRNA lipoplexes with N/P 0.35 were constant as a function of incubation time, while those of DE-DOPE/miRNA lipoplexes prepared at higher N/P ratios did not change up to 2 days, with a slight increase at day 7.

DF/miRNA lipoplexes were stable up to 7 days, maintaining an approximately constant average hydrodynamic diameter of 273–295 nm and PDI of 0.26–0.36. Z-potential remained

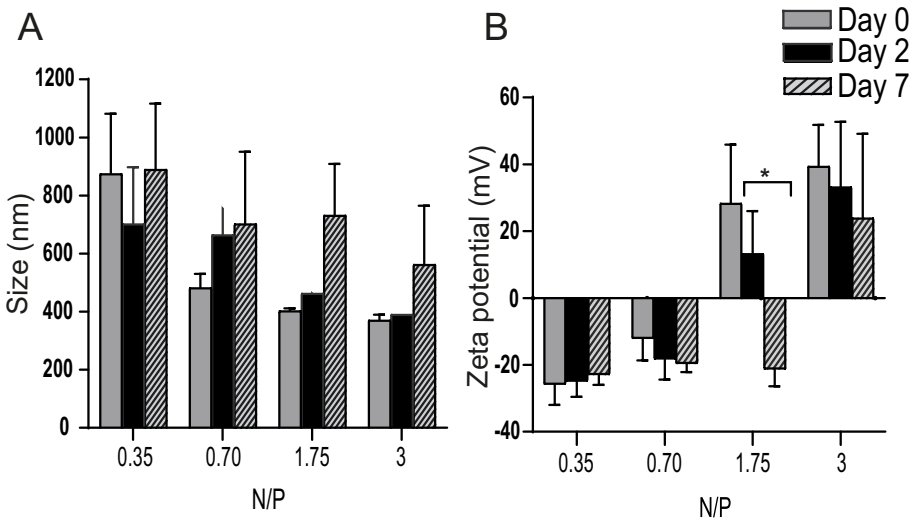

Fig. 2. Stability study under storage conditions (4 °C) of DE-DOPE/miRNA lipoplexes evaluated overtime at different N/P ratios: (A) hydrodynamic diameter and (B) Zeta potential of lipoplexes. NegmiR was loaded as model miRNA. Data are expressed as mean ± SD. Statistical analysis was performed by 1-way ANOVA.

positive with a decrease at day 2 and no further variation at day 7 (Table 2).

Overall, results suggested that stability to short-term storage conditions of DE-DOPE/miRNA lipoplexes was enhanced by increasing the N/P ratio, with optimal results achieved at N/P 3.

Based on the enhanced stability, lower PDI and comparable size and zeta potential respect to the commercial DF-based formulation, DE-DOPE/miRNA lipoplexes with N/P 3 were selected for further experiments, aimed at comparing their physicochemical characteristics and biological effects with those of DF/miRNA lipoplexes.

Characterization of the optimized lipoplexes formulation

Morphology and loading efficiency

Morphological analysis of DE-DOPE liposomes and lipoplexes was carried out by cryo-TEM microscopy. Fig. 3A-B report representative cryo-TEM images of DE-DOPE liposomes and DE-DOPE/miRNA lipoplexes at the selected N/P ratio (N/P 3), respectively. Both particles showed spherical shape and nanoscale size. Particularly, the core of DE-DOPE/miRNA lipoplexes was denser compared to the shell, suggesting miRNA loading. Moreover, compared to DE-DOPE liposomes, DE-DOPE/miRNA lipoplexes showed a reorganization of DE-DOPE lipids in the presence of miRNA (Fig. 3B).[37]

LE of miRNA in DE-DOPE lipoplexes, evaluated by Qubit fluorometric quantification was 99 %, significantly higher than for DF/miRNA lipoplexes (64 % ± 1.4, $p < 0.0001$) (Fig. 3C).

MiRNA loading in DE-DOPE/miRNA lipoplexes was also qualitatively investigated by analysing the presence of unloaded miRNA in the supernatant after lipoplex preparation by gel electrophoresis (Fig. 3D). The absence of miRNA signal in the supernatant lane from DE-DOPE/miRNA lipoplexes confirmed that miRNA was completely loaded. On the contrary, a weak miRNA fluorescent band was observed in the electrophoretic lane of the supernatant from DF/miRNA lipoplexes, indicating the presence of unloaded miRNA. This finding confirms the lower loading efficiency of DF/miRNA lipoplexes. No signal was detected in the supernatant lanes from blank DE-DOPE and DF liposome controls (Fig. 3D).

Stability under physiological conditions

The physicochemical stability of optimized DE-DOPE/miRNA lipoplexes was evaluated at 37 °C in Milli-Q water, by measuring the hydrodynamic diameter, PDI and *Z*-potential over 48 h (Fig. 4 and Supplementary Table S6).

Results showed that DE-DOPE/miRNA lipoplexes were stable up to 6 h, with an average hydrodynamic diameter of 358 nm. A size increase up to 495 nm was observed at 24 h (although not significant), while PDI value remained stable at 0.2 (Supplementary Table S6). The size of DE-DOPE/miRNA lipoplexes significantly increased after 48 h, reaching a value of 783 nm ($p < 0.0001$). The average *Z*-potential of DE-DOPE/lipoplexes decreased as a function of incubation time from 48 mV to 21 mV after 6 h ($p < 0.0001$), reaching a negative value of −9 mV at 24 h ($p < 0.0001$) and − 18 mV at 48 h ($p < 0.0001$).

In contrast, DF/miRNA lipoplexes showed an approximately constant hydrodynamic diameter between 292 ± 19 nm and 312 ± 9 nm up to 24 h, while the Z-potential progressively decreased as a function of the incubation time, from 50 ± 0.5 mV to 35 ± 3 mV after 6 h ($p = 0.0364$) and 17 ± 3 mV after 24 h (p value <0.0001), reaching a negative value at 48 h (−2 ± 1 mV).

Results on lipoplex stability in Milli-Q water at 37 °C, particularly the Z-potential trend, suggested that DE-DOPE/miRNA lipoplexes could disassemble earlier (between 6 h and 24 h) as compared to DF/miRNA lipoplexes (between 24 h and 48 h), facilitating miRNA release.[37]

Table 2
Stability under storage conditions (4 °C in Milli-Q water) for DF/miRNA lipoplexes evaluated by dynamic light scattering analysis, measuring hydrodynamic size, *Z*-potential and PDI. NegmiR was loaded as model miRNA.

DF/miRNA	Size (nm)	PDI	Zeta potential (mV)
Day 0	273 ± 25	0.33 ± 0.09	54 ± 4
Day 2	291 ± 42	0.36 ± 0.20	25 ± 1
Day 7	295 ± 46	0.26 ± 0.02	20 ± 13

Release profile of miRNA

MiRNA release studies indicated a similar miRNA release behaviour from DE-DOPE/miRNA and DF/miRNA lipoplexes up to 6 h. However, at 8 h DE-DOPE/miRNA lipoplexes released a significantly higher amount of miRNA compared to DF/miRNA lipoplexes (89 % *vs.* 51 %, $p < 0.0001$) (Fig. 5A). From 8 h to 48 h, the amount of miRNA released from DE-DOPE/miRNA and DF/miRNA lipoplexes progressively increased, reaching 99 % and 82 % at 48 h ($p < 0.0001$).

miRNA released from DE-DOPE/miRNA and DF/miRNA lipoplexes was also analyzed by gel electrophoresis, by testing the miRNA content in the supernatant after 6 h, 8 h and 12 h of incubation (Fig. 5B). The intense fluorescent band in the DE-DOPE/miRNA lipoplexes (lanes 3 and 5) confirmed a significantly higher release after 6 h. On the contrary, only a weak miRNA fluorescent band was observed for DF/miRNA lipoplexes (lanes 4 and 6) at 8 h and 12 h, confirming the delayed miRNA release from the commercial lipoplexes.

Characterization of DE-DOPE/miRcombo and DF/miRcombo lipoplexes

Both lipoplexes were then loaded with the four reprogramming miRNAs combination, called miRcombo (miRs-1, 133, 208 and 499) and characterized for their size, Z-potential, PDI and LE, before *in vitro* cell tests.

As shown in Table 3, DE-DOPE/miRcombo lipoplexes exhibited a mean size of 405 ± 13 nm, a positive average *Z*-potential of 43 ± 1 mV and a low PDI value of 0.22 ± 0.03. As a comparison, DF/miRcombo lipoplexes showed a hydrodynamic diameter of 356 ± 52 nm, an average Z-potential of 41 mV and a low PDI value of 0.29. Furthermore, LE was 99.0 ± 0.2 % for DE-DOPE/miRcombo lipoplexes and 69 ± 5 % for DF/miRcombo lipoplexes ($p < 0.0001$). Hence, the loading of one or four different miRNAs (miRcombo) at the same (overall) dose did not influence LE, hydrodynamic size, PDI and Z-potential of both types of lipoplexes (Fig. 1, Fig. 3, Supplementary Table S2 and Table S3, Table 3).

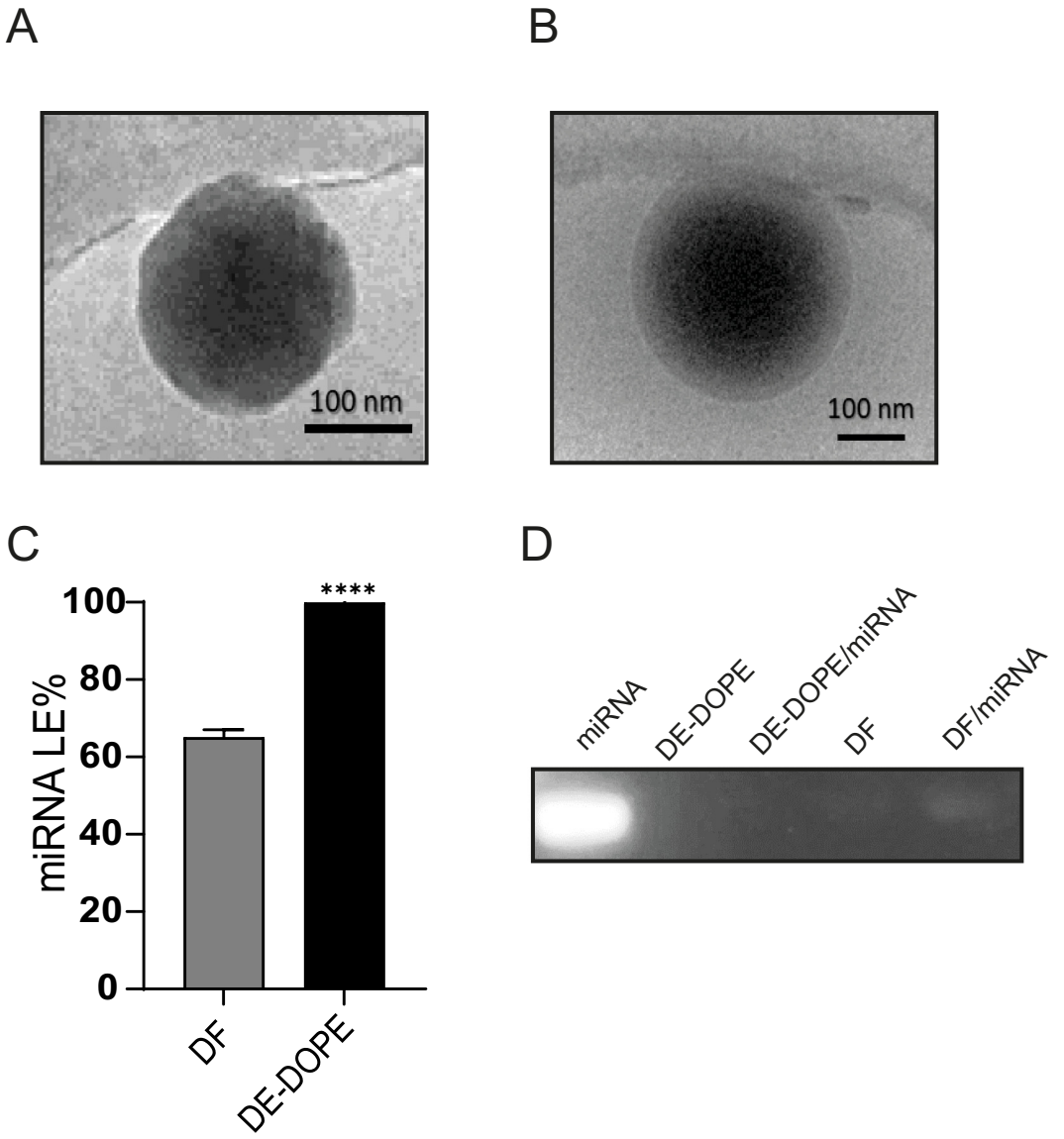

Fig. 3. Representative Cryo-TEM images of: (A) DE-DOPE liposomes and (B) DE-DOPE/miRNA lipoplexes. (C) MiRNA loading efficiency (LE) measured by Qubit fluorimetric quantification assay [t-test analysis, $p < 0.05$]. (D) Detection of unloaded miRNA in the supernatant of DE-DOPE/miRNA (N/P 3) and DF/miRNA lipoplexes by Agarose gel electrophoresis. Lanes represent: control miRNA solution (5 μM); empty DE-DOPE liposomes; supernatant from DE-DOPE/miRNA lipoplexes; empty DF liposomes; supernatant from DF-miRNA lipoplexes. NegmiR was loaded as a model miRNA. Statistical analysis was performed by t-test.

In vitro studies

In vitro cytocompatibility of liposomes and lipoplexes

Preliminary *in vitro* cell tests were performed using AHCFs and lipoplexes loaded with miR-1 to assess their cytocompatibility. AHCFs were transfected for 24 h and cytocompatibility was evaluated after 24 h and 48 h culture times.

As shown in Supplementary Fig. S2, both DE-DOPE liposomes and DE-DOPE/miRNA-1 lipoplexes did not elicit cytotoxicity *in vitro* at the tested concentrations with cell viability percentage comparable to untreated controls. On the other hand, the viability of cells treated with DF liposomes or DF/miRNA lipoplexes was significantly reduced to 60 % at 24 h (*i.e.*, immediately at the end of transfection treatment).

Fig. 6 compares the cytocompatibility of DF/miRNA and DE-DOPE/miRNA lipoplexes at two concentrations (DE-DOPE/miRNA_100 and DE-DOPE/miRNA_65) after 24 h (*i.e.*, at the end of transfection) and 48 h (*i.e.*, 24 h after the end of transfection). DE-DOPE/miRNA_100 corresponds to DE-DOPE/miRNA lipoplexes formulated with the same initial miRNA amount as DF/miRNA lipoplexes. As DF/miRNA lipoplexes loaded around 65 % of the initial miRNA, DE-DOPE/miRNA_65 formulation was also tested, corresponding to 65 % of DE-DOPE/miRNA_100 formulation and carrying the same miRNA amount as DF/miRNA lipoplexes.

Viability of AHCFs treated with DF/miRNA was lower at both timepoints, with a significantly lower value of 60 % at 24 h. On the contrary, AHCFs treated with DE-DOPE/miRNA

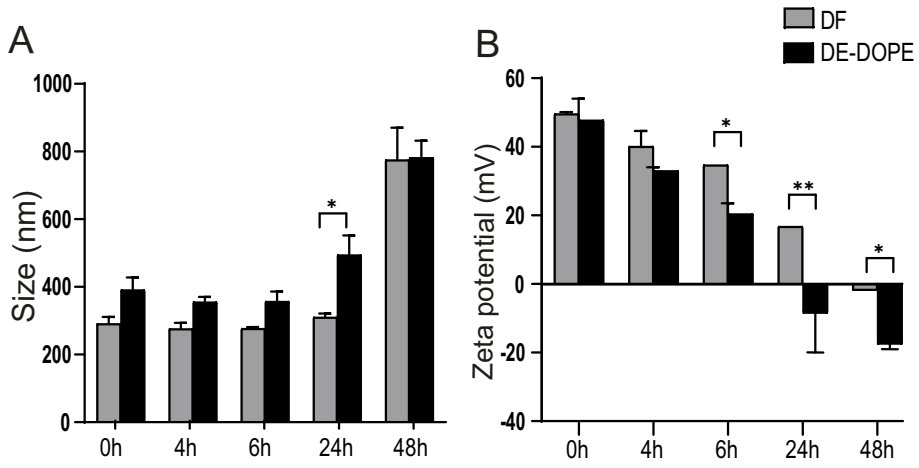

Fig. 4. Stability study at physiological temperature by measuring: (A) Size and (B) Zeta potential of DE-DOPE/miRNA lipoplexes at N/P 3 as a function of their incubation time (0, 4, 6, 24 and 48 h) compared to DF/miRNA lipoplexes. Data are expressed as mean ± SD. NegmiR was loaded as model miRNA. Statistical analysis was performed by 1-way ANOVA.

lipoplexes showed 80–100 % cell viability at both timepoints, confirming the higher cytocompatibility of DE-DOPE formulations. DE-DOPE/miRNA_65 showed superior cytocompatibility at 24 h, while no differences were detected between DE-DOPE/miRNA_100 and DE-DOPE/miRNA_65 formulations at 48 h. Cell viability of transfected AHCFs was observed also using bright field microscopy at 24 h (*i.e.*, at the end of transfection treatment) (Fig. 6B). While AHCFs transfected with DE-DOPE/negmiR lipoplexes appeared flattened and elongated as control cells, AHCFs transfected with DF/negmiR lipoplexes showed evident morphological changes with rounded shape, consistent with dead or dying fibroblasts.

In vitro miRNA uptake by AHCFs

The ability of DE-DOPE/miRNA lipoplexes to favor miRNA uptake by AHCFs, compared to commercial DF/miRNA lipoplexes was evaluated using FAM-labeled miR-1 (Fig. 7).

A significantly higher percentage of FAM^+ cells was observed for AHCFs transfected with DE-DOPE/miRNA_100 lipoplexes (~99 % FAM^+ cells) compared to DF/miRNA transfected AHCFs after 12 h transfection (~93 % FAM^+ cells). AHCFs transfected with diluted DE-DOPE/miRNA formulations, namely DE-DOPE/miRNA_65 and DE-DOPE/miRNA_50, showed ~92 % of FAM^+ cells with no significant difference respect to DF/miRNA formulation, whereas the more diluted DE-DOPE/miRNA_25 formulation achieved nearly 78 % of FAM^+ cells after 12 h transfection (Fig. 7B). Therefore, DE-DOPE/miRNA_100 lipoplexes showed a significantly higher internalization efficiency than DF/miRNA lipoplexes, while DE-DOPE/miRNA lipoplexes at lower concentrations (DE-DOPE/miRNA_65 and DE-DOPE/miRNA_50) showed comparable uptake efficiency to DF/miRNA lipoplexes. Further decrease in the concentration of DE-DOPE/miRNA lipoplexes also decreased uptake efficiency.

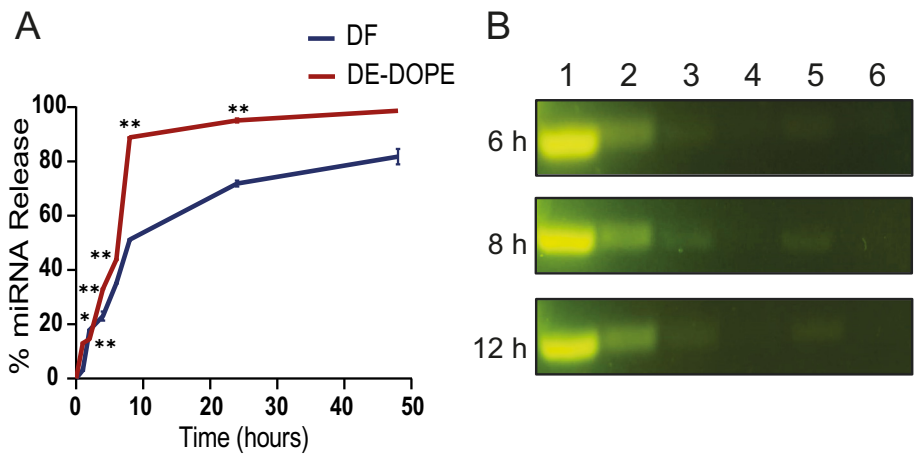

Fig. 5. (A) Release profile of miRNA from DE-DOPE/miRNA lipoplexes (N/P 3) (red line) and DF/miRNA lipoplexes (blue line), as a function of their incubation time (1, 2, 3, 4, 6, 8, 24 and 48 h) at 37 °C in 10 mM PBS. Data are expressed as mean ± SD. [ANOVA analysis, p value summary: * $p < 0.05$; ** $p < 0.001$]. (B) Detection of released miRNA from miRNA-loaded lipoplexes at 6, 8, and 12 h by Agarose gel electrophoresis. Lanes represent: 1) 50 μM miRNA and 2) 5 μM miRNA (control); 3) and 5) DE-DOPE/miRNA lipoplexes; and 4) and 6) DF-miRNA lipoplexes.

Table 3
Hydrodynamic diameter, PDI and Zeta potential measured by DLS analysis and quantification of miRcombo LE for DE-DOPE/miRcombo and DF/miRcombo lipoplexes. Data are expressed as mean ± SD.

	Size (nm)	PDI	Zeta potential (mV)	miRcombo LE (%)
DE-DOPE/miRcombo	405 ± 13	0.22 ± 0.03	43 ± 1	99.0 ± 0.2
DF/miRcombo	356 ± 52	0.29 ± 0.04	41 ± 10	69.0 ± 5.0

In agreement with the uptake efficiency results, DE-DOPE/miRNA_100-transfected AHCFs showed significantly higher average fluorescence intensity compared to all conditions after 12 h transfection (Fig. 7C). This result further evidenced the higher amount of miRNA delivered to AHCFs by DE-DOPE/miRNA respect to DF/miRNA lipoplexes due to their higher efficiency of miRNA loading and release.[45]

In vitro miRNA uptake and transfection ability and miRcombo direct reprogramming of AHCFs into iCMs

Next, we investigated whether lipoplexes were able to deliver functional miRNAs into AHCFs and to induce fibroblast reprogramming into iCMs (Fig. 8A). Among all cardiac-specific miRNAs, we investigated the delivery of miR-1 mediated by DF/miR-1 and DE-DOPE/miR-1 lipoplexes. MiR-1 is one of the most abundant miRNAs in the human heart and its expression is higher in cardiomyocytes, but not in fibroblasts. Moreover, TWF-1, which is involved in cardiac hypertrophy, has been assessed as a direct target of miR-1 in cardiac fibroblasts.[46] Therefore, we transfected AHCFs with DF/miR-1 and DE-DOPE/miR-1 lipoplexes and evaluated miR-1 internalization and TWF-1 mRNA expression, using ddPCR analysis. Non-transfected and negmiR-transfected cells were used as controls. After 48 h of culture, fold change expression of miR-1 in DE-DOPE/miR-1 transfected cells (miR-1, 25 nM) was significantly higher (~950) than DF/miR-1 transfected cells (~420) compared to controls ($p < 0.0001$) (Fig. 8B). These results confirm higher miR-1 delivery efficiency of DE-DOPE/miR-1 compared to DF/miR-1 lipoplexes, due to their superior loading efficiency.

Next, we analyzed TWF-1 mRNA target downregulation after 48 h culture time in both DF/miR-1 and DE-DOPE/miR-1 transfected cells. Fold change of TWF-1 expression was significantly decreased in all cases compared to controls (Fig. 8C), but

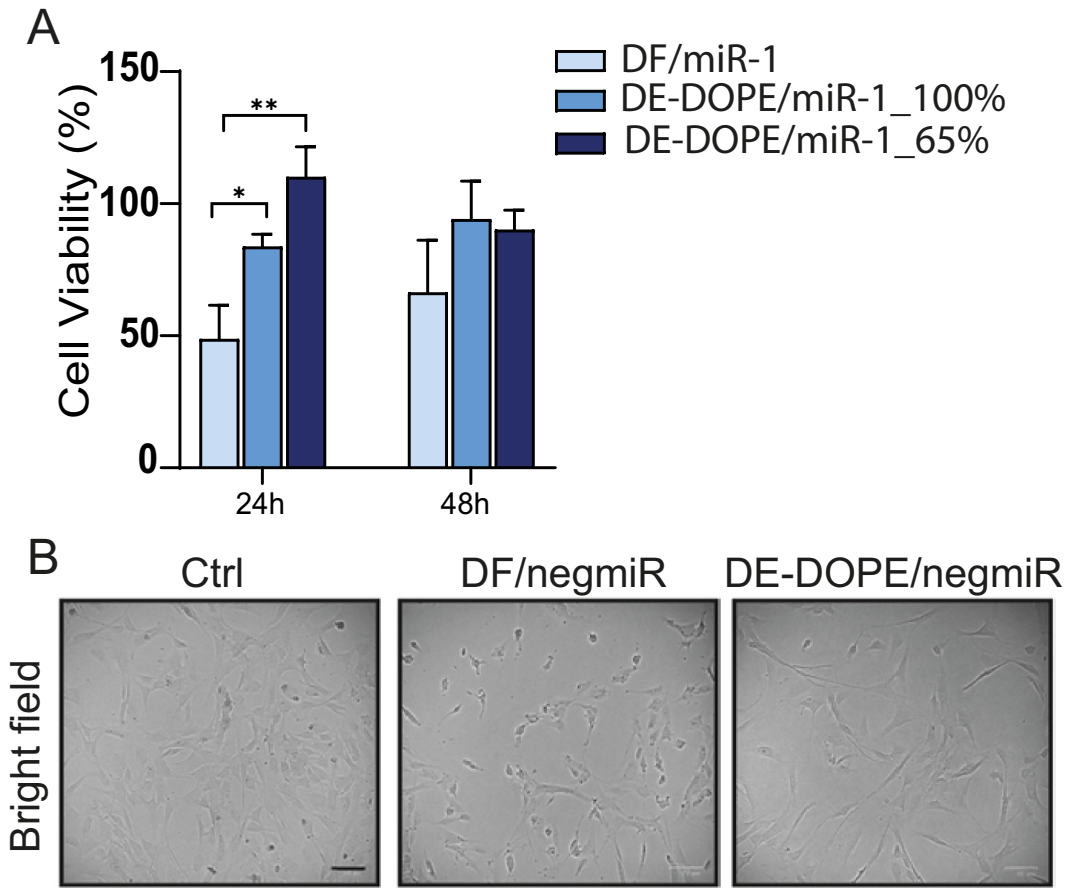

Fig. 6. (A) Viability of AHCFs transfected for 24 h with DF/miR-1 and DE-DOPE/miR-1 lipoplexes. DE-DOPE/miR-1 lipoplexes were tested at two concentrations: DE-DOPE/miRNA_100 (as prepared), DE-DOPE/miRNA_65 (65 % of the previous formulation, loading the same miRNA amount as DF/miRNA lipoplexes). Cell viability was analyzed at 24 h and at 48 h by resazurin assay. Viability of transfected AHCFs was normalized to non-transfected AHCFs. Cell viability after 24 h varied significantly between DF and DE-DOPE based lipoplexes at both concentrations (*$p = 0.0115$ and **$p = 0.0035$). (B) Brightfield microscopy images of AHCFs transfected with negmiR using DF and DE-DOPE based lipoplexes after 24 h. Scale bar = 100 μm.

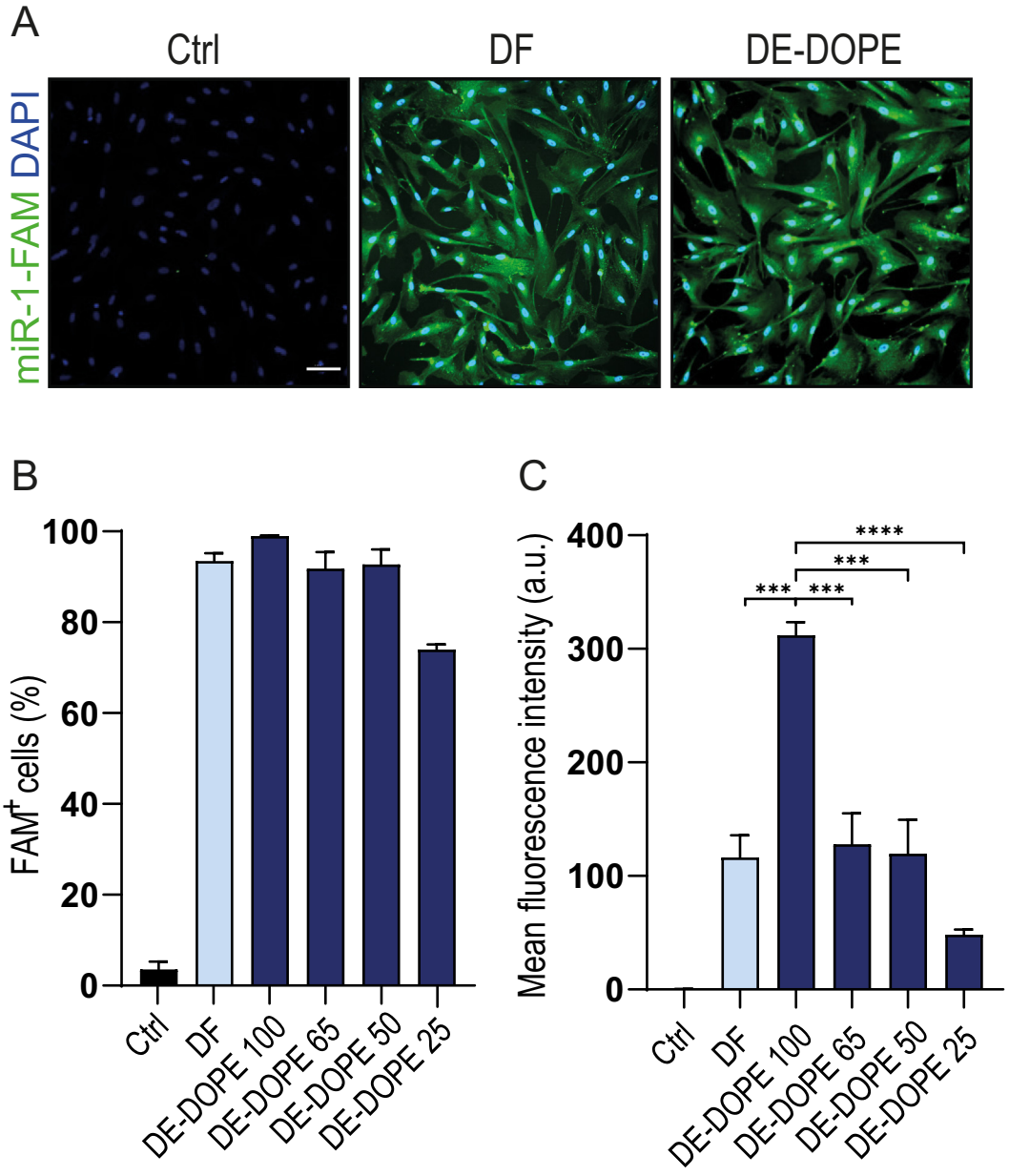

Fig. 7. miRNA internalization in AHCFs mediated by DF/miRNA and DE-DOPE/miRNA lipoplexes: (A) representative fluorescence microscopy images showing FAM-labeled miR-1 uptake by AHCFs, mediated by DF/miRNA and DE-DOPE/miRNA after 12 h transfection. Non-transfected cells were used as control. Nuclei were counterstained with DAPI (blue). Scale bar =100 μm. (B) Flow cytometric analysis reporting the percentage of FAM-labeled miR-1 positive cells (FAM^+ cells) transfected with DF/miRNA or DE-DOPE/miRNA (12 h transfection). Data represent mean values of triplicates ± SD from three independent experiments. (C) Mean fluorescence intensity of FAM-labeled miR-1 positive AHCFs after 12 h transfection with DF/miRNA and DE-DOPE/miRNA. Data represent mean values of triplicates ± SEM from three independent experiments.

no significant differences were detected between DE-DOPE/miR-1 and DF/miR-1 lipoplexes.

Then, the ability of DE-DOPE-based lipoplexes to influence miRcombo-mediated direct reprogramming of AHCFs into iCMs was analyzed by transfecting AHCFs with miRcombo using DF/miRcombo and DE-DOPE/miRcombo lipoplexes. After 7 days, the expression of GATA4 and MEF2C cardiomyocyte TFs (Fig. 8E-F) was found significantly increased in miRcombo-transfected compared to negmiR-transfected AHCFs using both DF or DE-DOPE based lipoplexes. However, DE-DOPE/miRcombo transfected cells showed significantly higher GATA4 ($p = 0.01$) and MEF2C ($p = 0.0001$) expression compared to DF/miRcombo lipoplexes. After 15 days, we analyzed the expression of cardiomyocyte markers TNNT2 and ACTC1. The expression of TNNT2, a gene encoding for cardiac Troponin T (cTnT), was significantly increased in miRcombo-transfected AHCFs using both lipoplexes (Fig. 8G and Supplementary Fig. S4). However, in DE-DOPE/miRcombo transfected cells TNNT2 expression was significantly higher ($p < 0.0001$) compared to DF/miRcombo transfected AHCFs, with ~9.6 fold

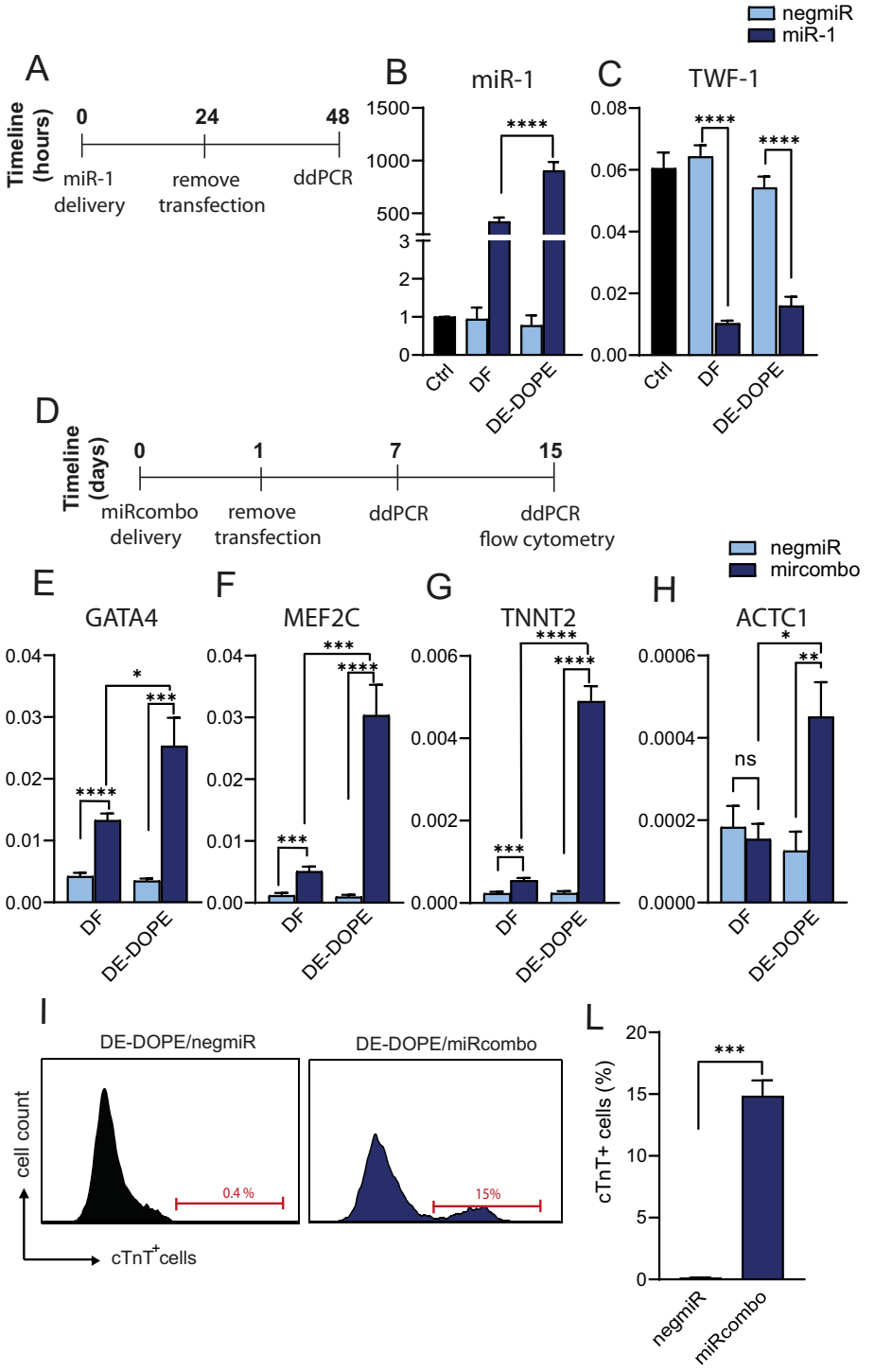

Fig. 8. *In vitro* transfection with miR-1 or miRcombo: (A) Timeline representation of miRNA transfection (miR-1) using DF or DE-DOPE based lipoplexes to assess miRNA delivery to AHCFs. (B) Levels of miR-1 in AHCFs transfected with negmiR or miR-1 using DF/miRNA and DE-DOPE/miRNA lipoplexes at 48 h as analyzed by ddPCR; (C) Gene expression of TWF-1 mRNA target in AHCFs transfected with negmiR or miR-1 using DF/miRNA and DE-DOPE/miRNA lipoplexes at 48 h as analyzed by ddPCR. MiRcombo direct reprogramming of AHCFs into iCMs. (D) Timeline representation of miRNA transfection (miRcombo) using DF or DE-DOPE based lipoplexes to assess AHCF reprogramming into iCMs -(E-H) Expression of GATA4 and MEF2C cardiac transcription factors at 7 days, TNNT2 and ACTC1 cardiomyocyte markers at 15 days for DE-DOPE/miRcombo and DF/miRcombo transfected AHCFs, evaluated by ddPCR. Reported data are average values ± SEM of three independent experiments. (I-L) Representative flow plots and percentage of cTnT+ cells in AHCFs transfected with negmiR or miRcombo using DE-DOPE based lipoplexes at 15 days. Reported data are average values ± SEM of three independent experiments. Statistical differences between the groups were determined with two-sided t-tests.

change expression compared to DF/miRcombo transfected cells. Interestingly, ACTC1 expression (Fig. 8H), which encodes for Actin Alpha Cardiac Muscle 1, was found significantly upregulated only in DE-DOPE/miRcombo transfected cells, showing increased expression compared to DF/miRcombo transfected cells ($p = 0.017$). Furthermore, flow cytometry analysis revealed ~15 % of cTnT+ cells in DE-DOPE/miRcombo transfected cells compared to DE-DOPE/negmiR cells (0.4 %) after 15 days of culture (Fig. 8I-L).

Discussion

The aim of the work was to design new biocompatible lipoplexes for efficient *in vitro* transfection of AHCFs with miRNAs for perspective applications in direct reprogramming of AHCFs into induced cardiomyocytes (iCMs).[29] Lipoplexes were formulated using an equimolar mixture of a cationic lipid (DE) and a fusogenic phospholipid (DOPE) (Supplementary Fig. S3). To the best of our knowledge, DE-DOPE lipoplexes have never been used for miRNA loading and release, although cationic lipids, such as DE, alone or in combination with fusogenic phospholipids, such as DOPE, have been previously applied in cancer gene therapy for plasmid DNA and siRNA delivery.[32,36,38,47] Previous reports have shown that DE-containing liposomes possess significantly lower cytotoxicity compared to Lipofectamine and have superior transfection efficiency *in vitro* compared to Lipofectin™ and ESCORT™ commercially available cationic lipid formulations.[32–38] Based on such findings, DE-DOPE/miRNA lipoplexes were here formulated and thoroughly characterized. DE-DOPE/miRNA lipoplexes with different ratio between the positively charged groups of the cationic lipid (N) and the negatively charged groups of miRNA (P) were produced *via* spontaneous electrostatic interactions. An increase in N/P ratio enhanced the electrostatic interactions and allowed the formation of lipoplexes with progressively smaller size and higher *Z*-potential, switching from negative to positive values (Fig. 1 and Supplementary Table S2), in agreement with previous findings.[38,48,49] Negative Z-potential values at N/P $\leq$ 0.70 suggested incomplete miRNA payload complexation, caused by the insufficient amount of positively charged groups.[48] Hence, N/P $\geq$ 1.75 was needed to obtain stable and monodisperse DE-DOPE/miRNA lipoplexes. Such results were confirmed by stability test of DE-DOPE/miRNA lipoplexes under short-term storage conditions (Fig. 2 and Supplementary Table S5). Such tests evidenced a progressive increase in lipoplex stability as a function of N/P ratio. Particularly, DE-DOPE/miRNA lipoplexes with N/P 3 maintained a positive surface charge with a minor increase in their hydrodynamic size only after 7 days of incubation in water at 4 °C (Fig. 2). Hence, DE-DOPE/miRNA lipoplexes with N/P 3 were selected for further investigations, and their physical and biological properties were compared to those of control lipoplexes based on DF, a widely used commercial transfection agent.[12,14,28] DE-DOPE/miRNA and DF/miRNA lipoplexes showed similar hydrodynamic size (372 ± 18 nm and 273 ± 25 nm, respectively) and Z-potential (40 ± 12 mV and 54 ± 14 mV, respectively) (Supplementary Figure S1 and Table S3). The positive surface charge is known to enhance the affinity of nanocarriers for the negatively-charged cell membrane, accounting for high cellular uptake.[50]

DE-DOPE/miRNA lipoplexes showed 99 % LE for both single miRNA and miRNA combination (miRcombo) *vs.* 64–69 % LE for DF/miRNA lipoplexes (Fig. 3C). Agarose gel electrophoresis confirmed the superior loading ability of DE-DOPE/miRNA lipoplexes (Fig. 3D). CryoTEM analysis of DE-DOPE liposomes and DE-DOPE/miRNA lipoplexes evidenced their spherical shape and confirmed their nanometric size (Fig. 3A, B). CryoTEM images of DE-DOPE/miRNA lipoplexes showed a dense core, evidencing successful loading of miRNA, and a lamellar structure, suggesting a reorganization of lipids due to the strong electrostatic interactions between the cationic lipid head groups and the phosphate groups in miRNA.[48]

DE-DOPE/miRNA lipoplexes disassembled earlier than DF/miRNA lipoplexes (Fig. 4), as indicated by the decreasing trend of the Z-potential as a function of the incubation time in physiological conditions (Milli-Q water, 37 °C), with Z-potential switching to a negative value after 24 h for DE-DOPE/miRNA lipoplexes, *vs.* 48 h for DF/miRNA lipoplexes[37] (Fig. 4B).

In agreement with these findings, DE-DOPE/miRNA lipoplexes released a significantly higher amount of miRNA payload after 6 h (90 %) reaching 100 % release after 48 h, while release of miRNAs from DF/miRNA lipoplexes was only 50 % after 6 h and reached 80 % after 48 h (Fig. 5). Considering that DF/miRNA lipoplexes loaded around 65 % of initial miRNA and released 80 % of their cargo after 48 h, the effective miRNA quantity released from DF/miRNA lipoplexes was around 50 % the amount released from DE-DOPE/miRNA lipoplexes. For this reason, different dilutions of DE-DOPE/miRNA lipoplex formulation were tested to assess their cytotoxicity and miRNA internalization ability by AHCFs (Fig. 6 and Supplementary Fig.S2). DF is commercialised as a transfection reagent for a wide range of applications and has been exploited to deliver different miRNAs to several cell types, such as miR-198 mimics to N/TERT-1 keratinocytes and miR-34/let-7 to non-small cell lung cancer (NSCLC), achieving favourable results.[27,51] Interestingly, DF is the most exploited transfection reagent for *in vitro* miRcombo release, for direct reprogramming of mouse fibroblasts into induced cardiomyocytes.[39,40,52–55] Additionally, Paoletti et al. have recently demonstrated direct reprogramming of adult human cardiac fibroblasts (AHCFs) into induced cardiomyocytes by using DF/miRcombo lipoplexes.[29] However, in this work, viability of AHCFs was found to be decreased after the administration of DF/miRNA lipoplexes below 70 % (Fig. 6A), which represents the threshold value for cytocompatibility according to ISO 10993. On the other hand, DE-DOPE/miRNA lipoplexes were cytocompatible (Fig. 6).

AHCFs were then transfected with DF/miR-1 or DE-DOPE/miR-1 lipoplexes for 24 h, and miR-1 endogenous expression was analyzed after 48 h culture time.[29] Given the superior LE and release ability of DE-DOPE/miRNA *vs.* DF/miRNA lipoplexes, miR-1 expression was around 2-fold higher in AHCFs transfected with DE-DOPE/miRNA *vs.* DF/miRNA lipoplexes (Fig. 8B). Target TWF-1 mRNA expression was significantly downregulated in AHCFs transfected with DE-DOPE/miR-1 lipoplexes, compared to DE-DOPE/negmiR lipoplexes and non-transfected control cells (Fig. 8C). However, no differences in

TWF-1 mRNA expression were observed in AHCFs transfected with DF/miR-1 and DE-DOPE/miR-1 lipoplexes, suggesting that the different levels of miR-1 delivered by the two transfection methods did not result in different TWF-1 mRNA downregulation. Hence, the amount of miR-1 delivered by both DF/miR-1 and DE-DOPE/miR-1 lipoplexes was sufficient to achieve significant target mRNA downregulation compared to controls. However, it is known that delivered miRNAs not only induce downregulation (*i.e.*, degradation) of target mRNAs but also inhibit mRNA mediated translation process.[6] Hence, higher miR-1 level in transfected AHCFs could inhibit target mRNA translation without causing mRNA degradation. Such effect could be elucidated by quantifying the expression of target proteins and was here indirectly demonstrated by analysing the direct reprogramming effect of miRcombo delivery to AHCFs by using the different lipoplexes.

Indeed, the high miRNA level mediated by DE-DOPE/miRNA lipoplexes could be particularly useful when combinatorial miRNA therapies are used, as in the case of miRcombo. The success of miRcombo-mediated direct reprogramming is strongly dependent on the efficient delivery of the four miRNAs. Recently multicistronic viral vectors were designed to highly express all miRNAs of miRcombo at stoichiometric level in neonatal mouse fibroblasts, demonstrating superior direct reprogramming efficiency respect to lentiviral vectors delivering the individual miRNAs of miRcombo, as well as to multicistronic viral vectors overexpressing single miRNAs of the four miRNA combination.[56] To prove that enhanced non-viral delivery of miRcombo can similarly improve direct reprogramming outcomes, we investigated the effect of DE-DOPE/miRcombo reprograming compared to DF/miRcombo one. The expression of GATA4 and MEF2C mRNA, after 7 days of culture, and TNNT2 and ACTC1 mRNA at 15 days was significantly higher for AHCFs transfected with DOPE/miRcombo than DF/miRcombo lipoplexes (Fig. 8E-H). Moreover, increased cell percentage positive for cTnT was observed in DE-DOPE/miRcombo transfected AHCFs compared to previously reported reprogramming efficiency (~11 % of $cTnT^+$ cells) using DF transfection (Fig. 8I-L).[29] Such findings suggest that increased cell viability and higher miRNA level delivered to AHCFs using DE-DOPE/miRcombo lipoplexes allowed more efficient direct cell reprogramming of AHCFs toward the iCM state.

To the best of our knowledge, only Kim et al. have attempted at optimizing miRcombo delivery for direct cardiac reprogramming, by testing both commercially available and modified nanosystems.[57] However, target cells were embryonic mouse fibroblasts which offer significantly inferior epigenetic resistance to direct cardiac reprogramming compared to AHCFs. Kim et al. found that the most effective transfection agent for miRcombo delivery to embryonic mouse fibroblasts was deoxycholic acid-conjugated poly(ethylene imine), due to its lowest cytotoxicity and highest transfection ability (50 %) among the tested nanosystems. Commonly, low direct reprogramming efficiency has been attributed to several molecular barriers, such as epigenetic modifications, epithelial-to mesenchymal transition (EMT) and transforming growth factor β (TGFβ) signaling, while the expression level of miRNAs has been rarely considered as a key factor in direct reprogramming outcomes.[56,58] Hence, the design of safe and efficient non-viral vectors for miRcombo delivery represents an under-appreciated factor for increasing the efficiency of direct cardiac reprogramming of AHCFs into induced cardiomyocytes. Herein, DE-DOPE/miRcombo lipoplexes showed the ability to efficiently deliver miRcombo to AHCFs, with preliminary evidence of enhanced direct cardiac reprogramming.

Interestingly, we have recently demonstrated that direct reprogramming efficiency significantly increases when miRcombo-transfected AHCFs (using DF/miRcombo lipoplexes) are cultured in 2D conditions in the presence of biomimetic proteins and, still more, in a 3D fibrin hydrogel containing cardiac biomatrix (a cardiac ECM produced *in vitro* by AHCFs), compared to their culture on uncoated 2D plates.[60] Based on these findings, further investigations will elucidate whether AHCFs transfected with DE-DOPE/miRcombo lipoplexes and cultured on uncoated *vs.* biomimetic protein-coated tissue culture plates and 3D biomimetic hydrogels may generate functional iCMs.[59] Indeed, the synergy between efficient cell transfection by biocompatible DE-DOPE/miRcombo lipoplexes and *in vitro* cell culture in a cardiac tissue-like microenvironment is expected to increase direct reprogramming efficiency and iCM maturation, respect to previous findings using DF/miRcombo.[60]

In conclusions, DE-DOPE/miRNA lipoplexes were demonstrated to be optimal lipid-based nanosystems for *in vitro* miRNA release as they are easy to assemble, have very high entrapment efficiency, are biocompatible and more efficiently release microRNAs (miR-1 and miRcombo) to AHCFs, compared to the commercial lipidic transfectant Dharmafect1. Further experiments evidenced higher efficiency of DE-DOPE/miRNA lipoplexes as non-viral vectors for *in vitro* miRcombo-mediated direct reprogramming of AHCFs into iCMs, compared to a commercially available control system. Future studies will elucidate the possibility to increase direct reprogramming efficiency and maturation level of reprogrammed cells at longer times in the presence of cardiac tissue-mimetic biochemical and biophysical stimuli.

Funding

This work was supported by the European Research Council (ERC) under the European Union's Horizon 2020 research and innovation programme (BIORECAR, grant agreement No. 772168, V.C.).

Availability of data and material

The datasets generated for this study are available on request to the corresponding author.

Authors' contributions

LN, CP, VC and CM designed the experimental part and analyzed the data. LN, BS, SA, IA, and CM conducted formulation and characterization of lipoplexes. CP and CD designed the *in vitro* culture experiments and ddPCR analysis. CP and GT conducted ddPCR analysis for lipoplexes cytocompatibility,

miR-1 overexpression and miRNA target downregulation. CP, CD, and CM conducted and supervised the *in vitro* culture experiments with adult human cardiac fibroblasts. VC, CM, BS, and SA supervised the work. VC acquired funding and supervised the project. The manuscript was written through main contributions by LN, CP, CM and VC and further help by all the authors. All authors have given approval to the final version of the manuscript.

CRediT authorship contribution statement

Letizia Nicoletti: Conceptualization, Investigation, Data curation, Writing – original draft. **Camilla Paoletti:** Conceptualization, Investigation, Data curation, Writing – original draft. **Giulia Tarricone:** Investigation. **Ilaria Andreana:** Investigation. **Barbara Stella:** Methodology, Visualization, Supervision. **Silvia Arpicco:** Methodology, Visualization, Supervision. **Carla Divieto:** Methodology, Visualization, Supervision. **Clara Mattu:** Conceptualization, Methodology, Writing – review & editing, Visualization, Supervision. **Valeria Chiono:** Conceptualization, Methodology, Supervision, Funding acquisition, Project administration, Writing – review & editing, Visualization.

Declaration of competing interest

There are no conflicts to declare.

Acknowledgements

This work was supported by the European Research Council (ERC) under the European Union's Horizon 2020 research and innovation programme (BIORECAR, grant agreement No. 772168, V.C.). We would like to acknowledge the contribution by Pierre-Yves Dugas (University of Lyon 1, C2P2 UMR 5265) for cryo-TEM observations at the "Centre Technologique des Microstructures" (CTμ - University of Lyon 1).

Appendix A. Supplementary data

Supplementary data to this article can be found online at https://doi.org/10.1016/j.nano.2022.102589.

References

1. Ghildiyal M, Zamore PD. Small silencing RNAs: an expanding universe. *Nat Rev Genet* 2009;**10**:94-108, https://doi.org/10.1038/nrg2504.
2. Lee Y, Jeon K, Lee JT, Kim S, Kim VN. MicroRNA maturation: stepwise processing and subcellular localization. *EMBO J* 2002;**21**:4663-70, https://doi.org/10.1093/emboj/cdf476.
3. Yong SL, Dutta A. MicroRNAs in cancer. *AnnuRevPatholMechDis* 2009;**4**:199-227, https://doi.org/10.1146/annurev.pathol.4.110807.092222.
4. Zhou SS, Jin JP, Wang JQ, Zhang ZG, Freedman JH, Zheng Y, et al. MiRNAS in cardiovascular diseases: potential biomarkers, therapeutic targets and challenges review-article. *Acta Pharmacol Sin* 2018;**39**:1073-84, https://doi.org/10.1038/aps.2018.30.
5. Liu NK, Xu XM. MicroRNA in central nervous system trauma and degenerative disorders. *Physiol Genomics* 2011;**43**:571-80, https://doi.org/10.1152/physiolgenomics.00168.2010.
6. Vidigal JA, Ventura A. The biological functions of miRNAs: lessons from in vivo studies. *Trends Cell Biol* 2015;**25**:137-47, https://doi.org/10.1016/j.tcb.2014.11.004.
7. Krützfeldt J. Strategies to use microRNAs as therapeutic targets. *Best Pract Res Clin Endocrinol Metab* 2016;**30**(5):551-61, https://doi.org/10.1016/j.beem.2016.07.004.
8. Muniyandi P, Palaninathan V, Mizuki T, Maekawa T, Hanajiri T, Mohamed MS. Poly(lactic-co-glycolic acid)/polyethylenimine nanocarriers for direct genetic reprogramming of microRNA targeting cardiac fibroblasts. *ACS ApplNano Mater* 2020;**3**:2491-505, https://doi.org/10.1021/acsanm.9b02586.
9. Ahir M, Upadhyay P, Ghosh A, Sarker S, Bhattacharya S, Gupta P, et al. Delivery of dual miRNA through CD44-targeted mesoporous silica nanoparticles for enhanced and effective triple-negative breast cancer therapy. *Biomater Sci* 2020;**8**:2939-54, https://doi.org/10.1039/d0bm00015a.
10. Lee SWL, Paoletti C, Campisi M, Osaki T, Adriani G, Kamm RD, et al. MicroRNA delivery through nanoparticles. *J Control Release* 2019;**313**:80-95, https://doi.org/10.1016/j.jconrel.2019.10.007.
11. Mattu C, Brachi G, Menichetti L, Flori A, Armanetti P, Ranzato E, et al. Alternating block copolymer-based nanoparticles as tools to modulate the loading of multiple chemotherapeutics and imaging probes. *Acta Biomater* 2018;**80**:341-51, https://doi.org/10.1016/j.actbio.2018.09.021.
12. Yang N. An overview of viral and nonviral delivery systems for microRNA. *IntJPharmInvestig* 2015;**5**:179-81, https://doi.org/10.4103/2230-973X.167646.
13. Fu Y, Chen J, Huang Z. Recent progress in microRNA-based delivery systems for the treatment of human disease. *ExRNA* 2019;**1**:1-14, https://doi.org/10.1186/s41544-019-0024-y.
14. Dasgupta I, Chatterjee A. Recent advances in miRNA delivery systems. *Methods Protoc* 2021;**4**:1-18, https://doi.org/10.3390/mps4010010.
15. Bessis N, GarciaCozar FJ, Boissier MC. Immune responses to gene therapy vectors: influence on vector function and effector mechanisms. *Gene Ther* 2004;**11**:S10-7, https://doi.org/10.1038/sj.gt.3302364.
16. Liu YP, Berkhout B. MiRNA cassettes in viral vectors: problems and solutions. *BiochimBiophysActaGene RegulMech* 1809;**2011**:732-45, https://doi.org/10.1016/j.bbagrm.2011.05.014.
17. Pal Singh P, Vithalapuram V, Metre S, Kodipyaka R. Lipoplex-based therapeutics for effective oligonucleotide delivery: a compendious review. *J Liposome Res* 2019;**30**:313-35, https://doi.org/10.1080/08982104.2019.1652645.
18. Martínez-Negro M, Sánchez-Arribas N, Guerrero-Martínez A, Moyá ML, de Ilarduya CT, Mendicuti F, et al. A non-viral plasmid DNA delivery system consisting on a lysine-derived cationic lipid mixed with a fusogenic lipid. *Pharmaceutics* 2019;**11**:1-11, https://doi.org/10.3390/pharmaceutics11120632.
19. Lonez C, Lensink MF, Kleiren E, Vanderwinden JM, Ruysschaert JM, Vandenbranden M. Fusogenic activity of cationic lipids and lipid shape distribution. *Cell Mol Life Sci* 2010;**67**:483-94, https://doi.org/10.1007/s00018-009-0197-x.
20. Mochizuki S, Kanegae N, Nishina K, Kamikawa Y, Koiwai K, Masunaga H, et al. The role of the helper lipid dioleoylphosphatidylethanolamine (DOPE) for DNA transfection cooperating with a cationic lipid bearing ethylenediamine. *BiochimBiophysActaBiomembr* 2013;**226**:412-8, https://doi.org/10.1016/j.bbamem.2012.10.017.
21. Ponti F, Campolungo M, Melchiori C, Bono N, Candiani G. Cationic lipids for gene delivery: many players, one goal. *Chem Phys Lipids* 2021;**235**105032, https://doi.org/10.1016/j.chemphyslip.2020.105032.
22. Scheideler M, Vidakovic I, Prassl R. Lipid nanocarriers for microRNA delivery. *Chem Phys Lipids* 2020;**226**, https://doi.org/10.1016/j.chemphyslip.2019.104837.
23. Deisseroth AR. Role of lipid-based and polymer-based non-viral vectors in nucleic acid delivery for next-generation gene therapy. *Exp Hematol* 1996;**24**:1053.
24. Wang T, Larcher LM, Ma L, Veedu RN. Systematic screening of commonly used commercial transfection reagents towards efficient

transfection of single-stranded oligonucleotides. *Molecules* 2018;**23**, https://doi.org/10.3390/molecules23102564.
25. Sluijter JPG, Van Mil A, Van Vliet P, Metz CHG, Liu J, Doevendans PA, et al. MicroRNA-1 and-499 regulate differentiation and proliferation in human-derived cardiomyocyte progenitor cells. *Arterioscler Thromb Vasc Biol* 2010;**30**:859-68, https://doi.org/10.1161/ATVBAHA.109.197434.
26. Zhao C, Sun G, Li S, Shi Y. A feedback regulatory loop involving microRNA-9 and nuclear receptor TLX in neural stem cell fate determination. *Nat Struct Mol Biol* 2009;**16**:365-71, https://doi.org/10.1038/nsmb.1576.
27. Sundaram GM, Common JEA, Gopal FE, Srikanta S, Lakshman K, Lunny DP, et al. 'See-saw' expression of microrna-198 and fstl1 from a single transcript in wound healing. *Nature* 2013;**495**:103-6, https://doi.org/10.1038/nature11890.
28. Remant RB, Thapa B, Valencia-Serna J, Aliabadi HM, Uludağ H. Nucleic acid combinations: a new frontier for cancer treatment. *J Control Release* 2017;**256**:153-69, https://doi.org/10.1016/j.jconrel.2017.04.029.
29. Paoletti C, Divieto C, Tarricone G, Di Meglio F, Nurzynska D, Chiono V. MicroRNA-mediated direct reprogramming of human adult fibroblasts toward cardiac phenotype. *<sb:contribution><sb:title>Front Bioeng</sb:title></sb:contribution><sb:host><sb:issue><sb:series><sb:title>Biotechnol</sb:title></sb:series></sb:issue></sb:host>* 2020;**8**:1-9, https://doi.org/10.3389/fbioe.2020.00529.
30. Michel T, Luft D, Abraham MK, Reinhardt S, Salinas Medina ML, Kurz J, et al. Cationic nanoliposomes meet mRNA: efficient delivery of modified mRNA using hemocompatible and stable vectors for therapeutic applications. *MolTherNucleic Acids* 2017;**8**:459-68, https://doi.org/10.1016/j.omtn.2017.07.013.
31. Jensen K, Anderson JA, Glass EJ. Comparison of small interfering RNA (siRNA) delivery into bovine monocyte-derived macrophages by transfection and electroporation. *Vet Immunol Immunopathol* 2014;**158**:224-32, https://doi.org/10.1016/j.vetimm.2014.02.002.
32. Arpicco S, Canevari S, Ceruti M, Galmozzi E, Rocco F, Cattel L. Synthesis, characterization and transfection activity of new saturated and unsaturated cationic lipids. *Farmaco* 2004;**59**:869-78, https://doi.org/10.1016/j.farmac.2004.06.007.
33. De Rosa G, De Stefano D, Laguardia V, Arpicco S, Simeon V, Carnuccio R, et al. Novel cationic liposome formulation for the delivery of an oligonucleotide decoy to NF-κB into activated macrophages. *Eur J Pharm Biopharm* 2008;**70**:7-18, https://doi.org/10.1016/j.ejpb.2008.03.012.
34. Surace C, Arpicco S, Dufaÿ-Wojcicki A, Marsaud V, Bouclier C, Clay D, et al. Lipoplexes targeting the CD44 hyaluronic acid receptor for efficient transfection of breast cancer cells. *Mol Pharm* 2009;**6**:1062-73, https://doi.org/10.1021/mp800215d.
35. Taetz S, Bochot A, Surace C, Arpicco S, Renoir JM, Schaefer UF, et al. Hyaluronic acid-modified DOTAP/DOPE liposomes for the targeted delivery of anti-telomerase siRNA to CD44-expressing lung cancer cells. *Oligonucleotides* 2009;**19**:103-15, https://doi.org/10.1089/oli.2008.0168.
36. Dufaÿ Wojcicki A, Hillaireau H, Nascimento TL, Arpicco S, Taverna M, Ribes S, et al. Hyaluronic acid-bearing lipoplexes: physico-chemical characterization and in vitro targeting of the CD44 receptor. *J Control Release* 2012;**162**:545-52, https://doi.org/10.1016/j.jconrel.2012.07.015.
37. Nascimento TL, Noiray M, Bourgaux C, Arpicco S, Taverna M, Cosco D, et al. *Supramolecular organization and siRNA binding of hyaluronic acid- coated lipoplexes for targeted delivery to the CD44 receptor*; 2015, https://doi.org/10.1021/acs.langmuir.5b01979.
38. Leite Nascimento T, Hillaireau H, Vergnaud J, Rivano M, Deloménie C, Courilleau D, et al. Hyaluronic acid-conjugated lipoplexes for targeted delivery of siRNA in a murine metastatic lung cancer model. *Int J Pharm* 2016;**514**:103-11, https://doi.org/10.1016/j.ijpharm.2016.06.125.
39. Dzau VJ, Jayawardena Tilanthi M, Finch Elizabeth A, Zhang Lunan, Zhang Hengtao, Hodgkinson Conrad P, et al. MicroRNA induced cardiac reprogramming in vivo evidence for mature cardiac myocytes and improved cardiac function. *Bone* 2005;**23**:1-7, https://doi.org/10.1161/CIRCRESAHA.116.304510.MicroRNA.
40. Jayawardena TM, Finch EA, Zhang L, Zhang H, Hodgkinson CP, Pratt RE, et al. MicroRNA induced cardiac reprogramming in vivo: evidence for mature cardiac myocytes and improved cardiac function. *Circ Res* 2015;**116**:418-24, https://doi.org/10.1161/CIRCRESAHA.116.304510.
41. Zhang H. Thin-film hydration followed by extrusion method for liposome preparation. *Methods Mol. Biol*. Humana Press Inc.; 2017. p. 17-22, https://doi.org/10.1007/978-1-4939-6591-5_2.
42. Yang H, Qin X, Wang H, Zhao X, Liu Y, Wo HT, et al. An in vivo miRNA delivery system for restoring infarcted myocardium. *ACS Nano* 2019;**13**:9880-94, https://doi.org/10.1021/acsnano.9b03343.
43. Ghasemzadeh N, Pourrajab F, Firoozabadi AD, Hekmatimoghaddam S, Haghiralsadat F, Cardiovascular Y, et al. *Ectopic microRNAs used to preserve human mesenchymal stem cell potency and epigenetics*, 14. ; 2018. p. 576-89.
44. Whale AS, Jones GM, Pavšič J, Dreo T, Redshaw N, Akyürek S, et al. Assessment of digital PCR as a primary reference measurement procedure to support advances in precision medicine. *Clin Chem* 2018;**64**:1296-307, https://doi.org/10.1373/clinchem.2017.285478.
45. Yang C, Hu R, Anderson T, Wang Y, Lin G, Law WC, et al. Biodegradable nanoparticle-mediated K-ras down regulation for pancreatic cancer gene therapy. *J Mater Chem B* 2015;**3**:2163-72, https://doi.org/10.1039/c4tb01623h.
46. Li Q, Song XW, Zou J, Wang GK, Kremneva E, Li XQ, et al. Attenuation of microRNA-1 derepresses the cytoskeleton regulatory protein twinfilin-1 to provoke cardiac hypertrophy (Journal of Cell Science 123, (2444–2452)). *J Cell Sci* 2010;**123**:2680, https://doi.org/10.1242/jcs.077578.
47. Liu C, Zhang L, Zhu W, Guo R, Sun H, Chen X, et al. Barriers and strategies of cationic liposomes for cancer gene therapy. *MolTher-Methods ClinDev* 2020;**18**:751-64, https://doi.org/10.1016/j.omtm.2020.07.015.
48. Nascimento TL, Hillaireau H, Noiray M, Bourgaux C, Arpicco S, Pehau-Arnaudet G, et al. Supramolecular organization and siRNA binding of hyaluronic acid-coated lipoplexes for targeted delivery to the CD44 receptor. *Langmuir* 2015;**31**:11186-94, https://doi.org/10.1021/acs.langmuir.5b01979.
49. Conejos-Sánchez I, Gallon E, Niño-Pariente A, Smith JA, De La Fuente AG, Di Canio L, et al. Polyornithine-based polyplexes to boost effective gene silencing in CNS disorders. *Nanoscale* 2020;**12**:6285-99, https://doi.org/10.1039/c9nr06187h.
50. He C, Hu Y, Yin L, Tang C, Yin C. Effects of particle size and surface charge on cellular uptake and biodistribution of polymeric nanoparticles. *Biomaterials* 2010;**31**:3657-66, https://doi.org/10.1016/j.biomaterials.2010.01.065.
51. Kasinski AL, Kelnar K, Stahlhut C, Orellana E, Zhao J, Shimer E, et al. A combinatorial microRNA therapeutics approach to suppressing non-small cell lung cancer. *Oncogene* 2015;**34**:3547-55, https://doi.org/10.1038/onc.2014.282.
52. Jayawardena TM, Egemnazarov B, Finch EA, Zhang L, Alan Payne J, Pandya K, et al. MicroRNA-mediated in vitro and in vivo direct reprogramming of cardiac fibroblasts to cardiomyocytes. *Circ Res* 2012;**110**:1465-73, https://doi.org/10.1161/CIRCRESAHA.112.269035.
53. Li Y, Dal-Pra S, Mirotsou M, Jayawardena TM, Hodgkinson CP, Bursac N, et al. Tissue-engineered 3-dimensional (3D) microenvironment enhances the direct reprogramming of fibroblasts into cardiomyocytes by microRNAs. *Sci Rep* 2016;**6**:1-11, https://doi.org/10.1038/srep38815.
54. Hu J, Hodgkinson CP, Pratt RE, Lee JW, Sullenger BA, Dzau VJ. Enhancing cardiac reprogramming via synthetic RNA oligonucleotides. *MolTherNucleic Acids* 2021;**23**:55-62, https://doi.org/10.1016/j.omtn.2020.10.034.

55. Dal-Pra S, Hodgkinson CP, Dzau VJ. Induced cardiomyocyte maturation: cardiac transcription factors are necessary but not sufficient. *PLoS One* 2019;**14**:1-18, https://doi.org/10.1371/journal.pone.0223842.
56. Kang MH, Hu J, Pratt RE, Hodgkinson CP, Asokan A, Dzau VJ. Optimizing delivery for efficient cardiac reprogramming. *Biochem Biophys Res Commun* 2020;**533**:9-16, https://doi.org/10.1016/j.bbrc.2020.08.104.
57. Hsu Shao, Yu B, Wang X, Lu Y, Schmidt CR, Lee RJ, et al. Cationic lipid nanoparticles for therapeutic delivery of siRNA and miRNA to murine liver tumor. *Nanomedicine: NBM* 2013;**9**:1169-80, https://doi.org/10.1016/j.nano.2013.05.007.
58. Talkhabi M, Zonooz ER, Baharvand H. Boosters and barriers for direct cardiac reprogramming. *Life Sci* 2017;**178**:70-86, https://doi.org/10.1016/j.lfs.2017.04.013.
59. Paoletti Camilla, Marcello Elena, Melis Maria Luna, Divieto Carla, Nurzynska Daria. Cardiac tissue-like 3D microenvironment enhances route towards human fibroblast direct reprogramming into induced cardiomyocytes by microRNAs _ Enhanced Reader.pdf. *Cells* 2022;**11**:800.
60. Paoletti C, Chiono V. Bioengineering methods in microRNA-mediated direct reprogramming of fibroblasts into cardiomyocytes. *FrontCardiovascMed* 2021;**8**, https://doi.org/10.3389/fcvm.2021.750438.